Environmental Science & Technology

Article

pubs.acs.org/est

Spectrophotometric Measurement of Calcium Carbonate Saturation States in Seawater

Regina A. Easley,[†] Mark C. Patsavas,[†] Robert H. Byrne,[†,*] Xuewu Liu,[†] Richard A. Feely,[+] and Jeremy T. Mathis[§]

[†]College of Marine Science, University of South Florida, St. Petersburg, Florida 33701, United States

[+]NOAA Pacific Marine Environmental Laboratory, Seattle, Washington 98115, United States

[§]School of Fisheries and Ocean Sciences, University of Alaska Fairbanks, Fairbanks, Alaska 99775, United States

Supporting Information

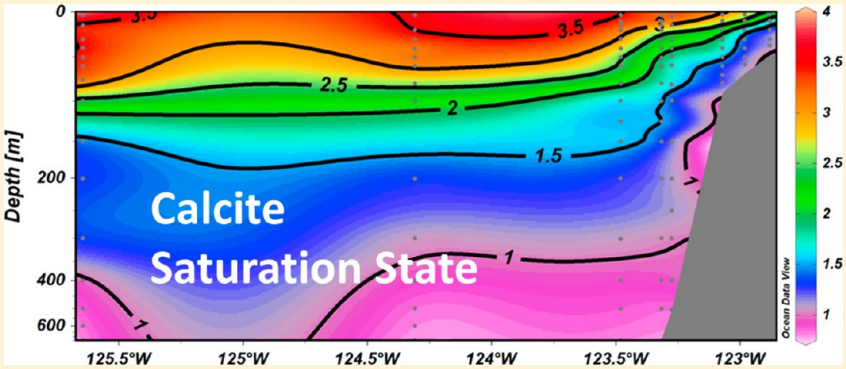

ABSTRACT: Measurements of ocean pH and carbonate ion concentrations in the North Pacific and Arctic Oceans were used to determine calcium carbonate saturation states (Ω_{CaCO_3}) from spectrophotometric methods alone. Total carbonate ion concentrations, $[CO_3^{2-}]_T$, were for the first time at sea directly measured using Pb(II) UV absorbance spectra. The basis of the method is given by the following:

$$-\log[CO_3^{2-}]_{Tspec} = \log\{({}_{CO3}\beta_1)/(e_2)\} + \log\{(R-e_1)/(1-Re_3/e_2)\}$$

where ${}_{CO}\beta_1$ is the $PbCO_3^0$ formation constant, e_i are molar absorptivity ratios, and $R = {}_{250}A/{}_{234}A$ (ratio of absorbances measured at 250 and 234 nm). On the basis of shipboard and laboratory Pb(II) data and complementary carbon-system measurements, the experimental parameters were determined to be (25 °C) the following:

$$\log\{({}_{CO3}\beta_1)/(e_2)\} = 5.513 - 5.358\times10^{-2}S + 5.166\times10^{-4}S^2$$
$$e_1 = 0.2293 - 5.554\times10^{-4}S + 8.440\times10^{-5}S^2$$
$$(e_3/e_2) = 3.091 - 8.730\times10^{-2}S + 9.363\times10^{-4}S^2$$

The resulting mean difference between the shipboard spectrophotometric and conventional determinations of $[CO_3^{2-}]_T$ was ±2.03 μmol kg^{-1}. The shipboard analytical precision of the Pb(II) method was ~1.71 μmol kg^{-1} (2.28%). Spectrophotometric $[CO_3^{2-}]_T$ and pH_T were then combined to calculate Ω_{CaCO_3}. For the case of aragonite, 95% of the spectrophotometric aragonite saturation states (Ω_{Aspec}) were within ±0.06 of the conventionally calculated values (Ω_{Acalc}) when $0.5 \le \Omega_A \le 2.0$. When $\Omega_A > 2.0$, 95% of the Ω_{Aspec} values were within ±0.18 of Ω_{Acalc}. Our shipboard experience indicates that spectrophotometric determinations of $[CO_3^{2-}]_T$ and Ω_{CaCO_3} are straightforward, fast, and precise. The method yields high-quality measurements of two important, rapidly changing aspects of ocean chemistry and offers capabilities suitable for long-term automated in situ monitoring.

Received: September 6, 2012
Revised: December 1, 2012
Accepted: December 2, 2012
Published: December 2, 2012

INTRODUCTION

Input of anthropogenic carbon dioxide (CO_2) to the oceans has reduced global surface seawater pH by approximately 0.1 since the preindustrial era.[1−3] Much research is currently focused on understanding the effects of a changing oceanic CO_2 system on marine organisms and ecosystems.[4−9] One result of the declining pH (i.e., ocean acidification) has been a decrease in the saturation states, Ω_{CaCO_3}, of the calcium carbonate ($CaCO_3$) polymorphs calcite and aragonite.[10−12] Saturation states can have species-specific physiological effects influencing, for example, calcification rates and productivity of the calcareous phytoplankton[13,14] that occupy the base of the oceanic food chain. Changes in Ω_{CaCO_3} are of particular concern in polar regions, where low-temperature waters more readily dissolve CO_2. The Arctic region, which supports economically important fisheries,[15,16] experiences seasonal aragonite undersaturation due to high primary productivity,[17] freshwater input from rivers and sea ice,[18] riverine delivery of terrigenous carbon,[19,20] and upwelling of corrosive older waters of Pacific origin.[21]

To determine seawater saturation states, total carbonate ion concentrations ($[CO_3^{2-}]_T$ = free carbonate + ion-paired carbonate) are typically calculated from the thermodynamic relations among $[CO_3^{2-}]_T$ and any two measurable CO_2 system parameters: dissolved inorganic carbon (DIC), pH, total alkalinity (TA), or CO_2 fugacity (fCO_2).[22] The most commonly used procedures require equipment that is expensive, commercially unavailable, or challenging to maintain.[23] The ability to directly measure $[CO_3^{2-}]_T$ using a single procedure, thereby creating a fifth independently measured CO_2 system parameter, would be highly beneficial.

The use of polymer-based electrodes[24,25] and direct examination of the UV spectrum of seawater[26] have been proposed for direct $[CO_3^{2-}]$ determination, but neither technique has been adopted for routine measurements. Another approach utilizes Pb(II) UV absorbance spectra,[27] which are responsive to the relative concentrations of (a) lead carbonate ($PbCO_3^0$), the dominant Pb(II) complex at high $[CO_3^{2-}]_T$, and (b) lead chloride species, which dominate at low levels of $[CO_3^{2-}]_T$ (Figure 1). Carbonate ion concentrations can be derived from measurements of the UV spectra plus knowledge of three experimental parameters related to molecularly based absorbance ratios and the equilibrium constant for the formation of lead carbonate species from an ensemble of lead chloride species ($PbCl^+$, $PbCl_2$, and $PbCl_3^-$). This method, analogous to the spectrophotometric determination of pH in seawater,[22] is fast, requires no calibration, and utilizes standard benchtop spectrometers, which are widely available and user-friendly.

In this study, field data collected during cruises in the northeast Pacific Ocean (August 2011) and the Arctic Ocean (October 2011) were used to assess and improve the method for using Pb(II) spectroscopy to measure carbonate ion concentrations ($[CO_3^{2-}]_T$) in seawater. Spectrophotometric concentrations directly measured at sea were compared with concentrations determined indirectly by conventional means (i.e., calculated from pH—DIC or pH—TA pairings). These comparisons were used to guide minor refinements to the original spectrochemical model.[27] At-sea precision of the method was assessed from replicate seawater samples. Finally, shipboard spectrophotometric pH_T−$[CO_3^{2-}]_T$ pairs were used to calculate in situ $CaCO_3$ saturation states, which were compared to saturation states calculated from pH_T−DIC or pH_T−TA.

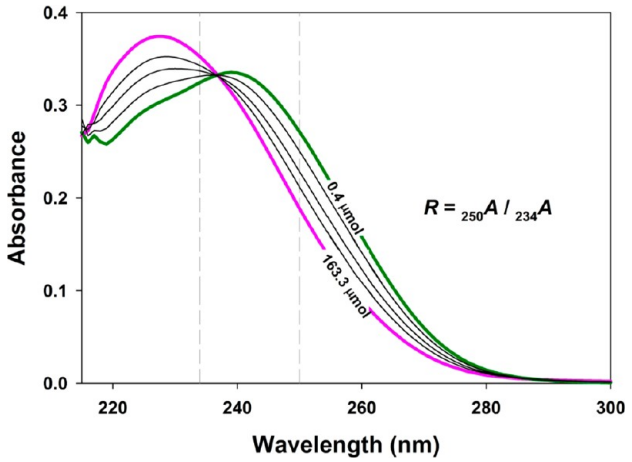

Figure 1. Pb(II) absorbance spectra in seawater at S = 35.7 and 25 °C for a range of carbonate ion concentrations, $0.4 \leq [CO_3^{2-}]_T \leq 163.3$ μmol kg^{-1}. The spectrum shown for 0.4 μmol kg^{-1} (green) indicates a predominance of lead chloride species, whereas the spectrum at 163.3 μmol kg^{-1} (pink) indicates primarily lead carbonate species. The wavelengths used to monitor the species are indicated by the dashed lines.

METHODS

Measurement of Standard CO_2 System Parameters. Discrete seawater samples were collected during oceanographic cruises in the Pacific Ocean (N = 1185, August 2011, *R/V Wecoma*, Cruise W1108C) and in the Beaufort Sea of the Arctic Ocean, (N = 305, October 2011, *USCGC Healy*, Cruise HLY1103) (Figure 2). The pH_T of each sample was determined spectrophotometrically using purified m-cresol purple, mCP (10 μL of 10 mmol kg^{-1} mCP in ∼30 mL of seawater) and 10 cm optical cells on an HP 8453 spectrometer.[28] For the U.S. West Coast samples, DIC was determined by coulometry.[22] For the Arctic samples, TA was determined by visible spectrometry.[29] Through the use of certified reference materials (CRMs), the DIC and TA measurements were demonstrated to be accurate to within 1 μmol kg^{-1} and 2 μmol kg^{-1}, respectively.[30] Phosphate and silicate concentrations were measured postcruise using an autoanalyzer.[31]

Spectrophotometric Measurement of Carbonate Ion Concentrations. Seawater samples were collected from Niskin bottles into 10 cm quartz cuvettes (∼30 mL volume) without exposure to the atmosphere. Each sample was thermostatted to 25 °C (±0.05), a UV blank was taken, and 100 μL of $PbCl_2$ (2.2 mM) was added. The $PbCl_2$ titrant had been prepared by dissolving lead chloride (Aldrich 99.999% purity, Lot 03114DE) in Milli-Q water. Absorbance A at two wavelengths (λ = 234 and 250 nm) was measured on an HP 8453 spectrometer, along with A at a nonabsorbing wavelength (350 nm). Whereas 234 nm is not the most sensitive wavelength to monitor $PbCO_3^0$ formation (Figure 1), it yields the most reproducible values[27] and lies outside the UV region strongly affected by CO_3^{2-} absorbance.[26] Total carbonate ion concentration is given by:

$$-\log[CO_3^{2-}]_{Tspec} = \log\{({}_{CO_3}\beta_1)/(e_2)\} + \log\{(R - e_1)/(1 - Re_3/e_2)\} \quad (1)$$

dx.doi.org/10.1021/es303631g | Environ. Sci. Technol. 2013, 47, 1468−1477

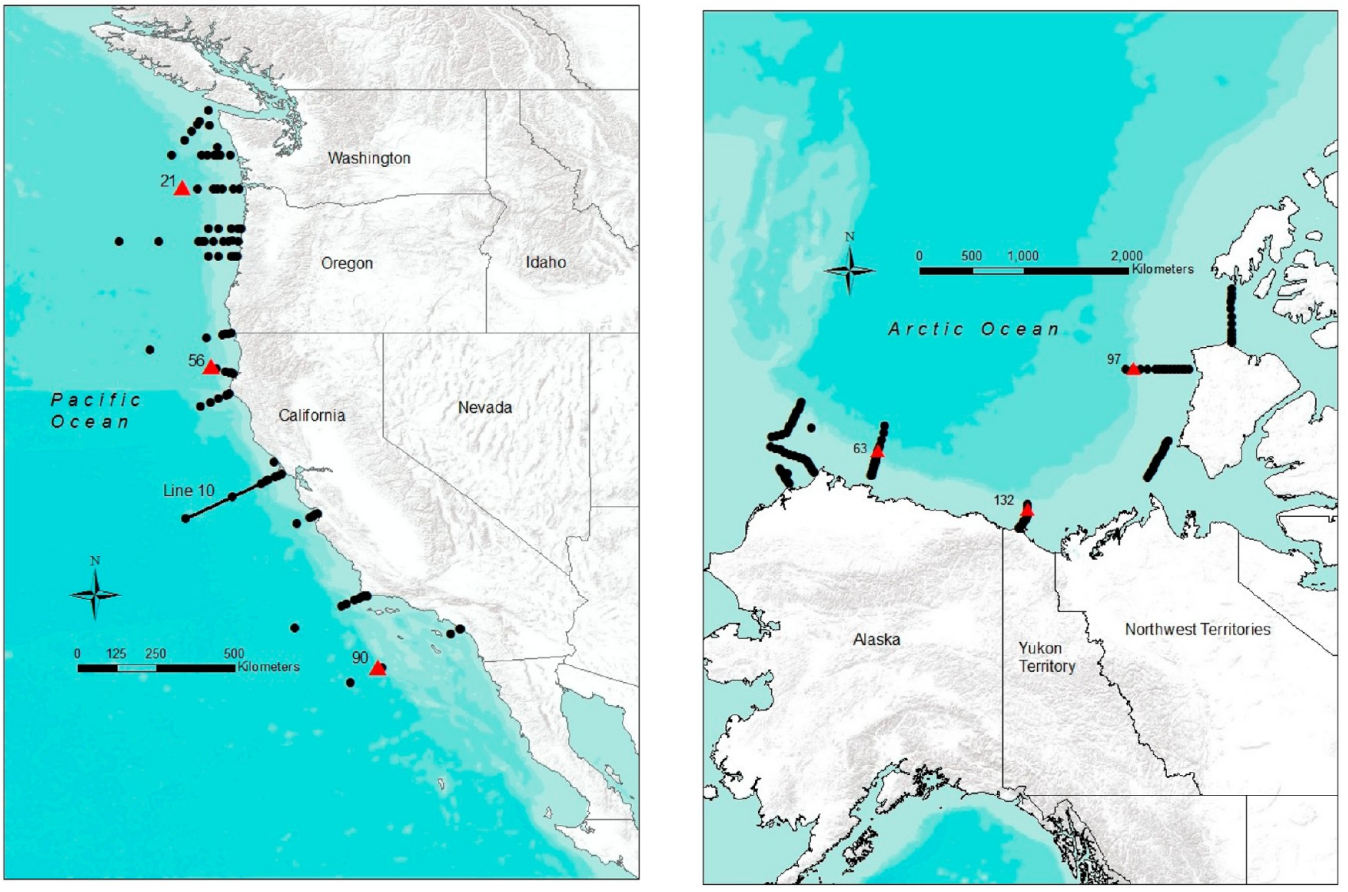

Figure 2. Hydrographic station locations. The U.S. West Coast seawater samples (N = 1185) were collected in August 2011, Arctic samples (N = 305) were collected in October 2011. The red triangles show the locations of the carbonate ion profiles shown in Figure 5. Contour plots of $CaCO_3$ saturation states for West Coast line 10 are shown in Figure 7.

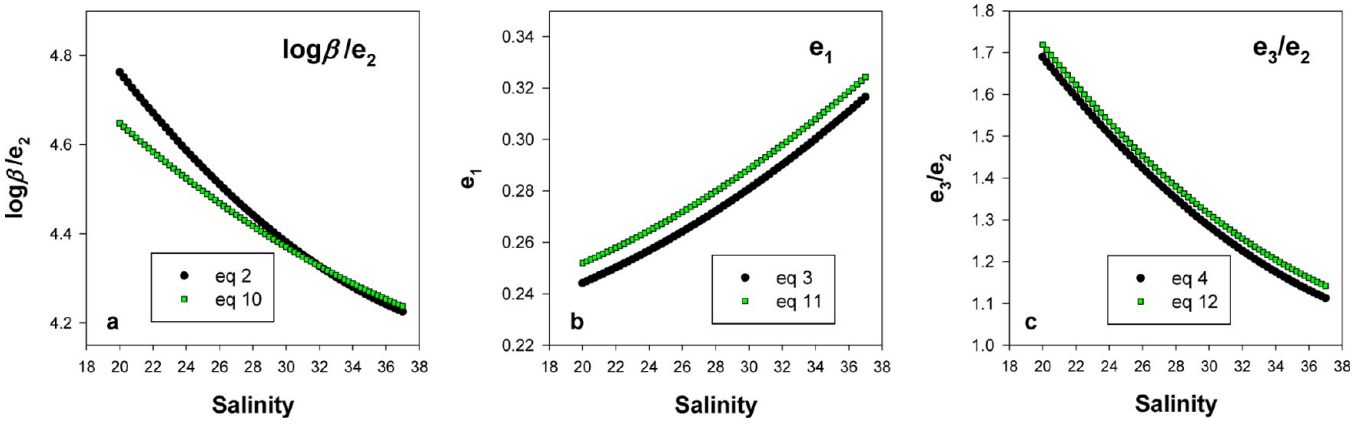

Figure 3. Salinity dependence of the three parameters required to determine $[CO_3^{2-}]_{Tspec}$ from eq 1. The original lab-based results (eqs 2–4, Byrne and Yao[27]) are shown in black. The optimized results (eqs 10–12, this study) are shown in green.

where ${}_{CO_3}\beta_1$ is the $PbCO_3^0$ formation constant, e_i are molar absorptivity ratios, and $R = {}_{250}A/{}_{234}A$.[27] (This equation is identical to eq 20 in Byrne and Yao[27]). The fitting parameters initially used for the 25 °C measurements were:

$$\log\{({}_{CO_3}\beta_1)/(e_2)\} = 6.087 - 8.495 \times 10^{-2}S + 9.360 \times 10^{-4}S^2 \quad (2)$$

$$e_1 = 0.2215 - 5.554 \times 10^{-4}S + 8.440 \times 10^{-5}S^2 \quad (3)$$

$$(e_3/e_2) = 3.061 - 8.730 \times 10^{-2}S + 9.363 \times 10^{-4}S^2 \quad (4)$$

where S is salinity.[27] The e_i terms are ratios of wavelength-specific molar absorptivity values (${}_{\lambda}\varepsilon$). The e_1 ratio is expressed in terms of the molar absorbance characteristics of $PbCO_3^0$, which is the dominating complex at high pH: $e_1 = {}_{250}\varepsilon_{PbCO_3}/{}_{234}\varepsilon_{PbCO_3}$. The e_3/e_2 term describes the absorbance ratios of lead in seawater at low pH (pH < 4.0), when $PbCO_3^0$ formation is insignificant and lead chloride species are strongly dominant: $e_3/e_2 = {}_{234}\varepsilon_{PbCl_x}/{}_{250}\varepsilon_{PbCl_x}$. The ratio e_2 is defined in

dx.doi.org/10.1021/es303631g | Environ. Sci. Technol. 2013, 47, 1468–1477

terms of the absorbance characteristics of both Pb(II) complexed with carbonate and Pb(II) complexed with chloride: $e_2 = {}_{250}\varepsilon_{PbCl_x}/{}_{234}\varepsilon_{PbCO_3}$.

Of the 1490 carbonate samples collected on the two cruises, 10 were determined to be outliers; 2 were rejected because of significant drift in the spectra (~0.01 absorbance units) and 8 were rejected because of baseline drift (>0.005 absorbance units). To assess measurement reproducibility, duplicate seawater samples were collected into separate quartz cells for a total of 171 pairs from the combined cruise data sets.

Determination of Carbonate Ion Perturbations. Small changes in sample carbonate ion concentration may occur due to the complexation of free CO_3^{2-} by Pb(II) from the $PbCl_2$ titrant. We assessed the extent of these potential carbonate perturbations using an approach similar to that used to determine pH perturbations upon addition of spectrophotometric dyes.[32] In the field, surface seawater samples were adjusted with HCl or NaOH to establish a range of carbonate ion concentrations. Pb(II) absorbance was then measured at two different concentrations of added $PbCl_2$ titrant: $\Delta R = R_{initial} - R_{final}$, where $R_{initial}$ is the absorbance ratio measured after addition of 100 μL of $PbCl_2$, and R_{final} is the value measured after a second 100 μL addition. Perturbation effects were also examined subsequently (postcruise) in the laboratory. A series of Gulf of Mexico seawater samples ($27 \geq S \geq 35$) over a range of carbonate ion concentrations were analyzed with the $PbCl_2$ titrants used on the West Coast and Arctic cruises. In agreement with Byrne and Yao,[27] no discernible perturbation trends were observed over a range of carbonate ion concentrations (Figure S1 of the Supporting Information). Perturbation corrections, which would include dilution effects, were therefore not applied to the measured absorbance ratios of eq 1.

Parameter Optimization. Total carbonate ion concentrations were calculated by conventional means ($[CO_3^{2-}]_{Tcalc}$) using CO2SYS[33] with inputs of pH_T and DIC for the West Coast samples and pH_T, TA, phosphate, and silicate for the Arctic samples. Modified Mehrbach et al.[34] constants, as refit by Dickson and Millero,[35] were used. A comparison of $[CO_3^{2-}]_{Tcalc}$ and $[CO_3^{2-}]_{Tspec}$ (eqs 1 and 2–4) showed that differences between the two quantities were nonrandom. The parameters of eqs 2–4 were therefore optimized (i.e., modified slightly) using *SigmaPlot* routines (Systat Software) to maximize internal consistency among the carbonate system parameters. Residuals of $[CO_3^{2-}]_T$ (conventional minus spectrophotometric concentrations) were used to guide the exercise. Goodness of fit was determined by examining the residual sum of squares with a running median averaged over intervals of 5 μmol kg^{-1}.

To generate the optimized model, changes were made to selected coefficients in eqs 2–4 to randomize the overall distribution of residuals. The constant term in the e_3/e_2 polynomial (eq 4) was varied to minimize residuals at low carbonate ion concentrations (i.e., near $[CO_3^{2-}]_T$ = 40 μmol kg^{-1}). The constant term in the e_1 polynomial (eq 3) was adjusted to minimize residuals for samples with $[CO_3^{2-}]_T$ >100 μmol kg^{-1}. This procedure was followed because e_3/e_2 most strongly influences carbonate ion calculations (eq 1) at low concentrations, whereas e_1 most strongly influences the calculations at high concentrations. In the $\log(\beta/e_2)$ expression (eq 2), all three polynomial terms were modified through simultaneous least-squares refinement of the coefficients to minimize the carbonate residual sum of squares for the entire data set. In summary, both laboratory[27] and field data were used to produce a model that maximizes the internal consistency between $[CO_3^{2-}]_{Tspec}$ and $[CO_3^{2-}]_{Tcalc}$.

Determination of in Situ Calcium Carbonate Saturation States. Calcium carbonate saturation states for in situ conditions can be determined from in situ calcium and carbonate ion concentrations at a given salinity, temperature, and pressure:

$$\Omega_{CaCO_3} = \frac{[Ca^{2+}][CO_3^{2-}]_T}{K_{SP}} \quad (5)$$

where K_{SP} is the $CaCO_3$ (calcite or aragonite) solubility product. Calcium behaves conservatively and can be obtained from $[Ca^{2+}] = 0.0102821\ S/35$. The quantity $[CO_3^{2-}]_T$ is not typically directly measured. To compute Ω_{CaCO3}, the CO2SYS[33] calculator uses inputs of any two conventional CO_2 system parameters (pH, TA, DIC, or fCO_2) to generate DIC and TA, which are invariant with temperature and pressure. From the resulting TA–DIC pair, saturation states for calcite (Ω_C) and aragonite (Ω_A) are then calculated for conditions of in situ temperature and pressure.

For the 2011 field data, in situ saturation states were calculated via two procedures: (a) using conventional CO_2 system measurements (pH_T–DIC or pH_T–TA) and (b) using spectrophotometric pH_T–$[CO_3^{2-}]_{Tspec}$. For the conventional calculations, CO2SYS input for the West Coast samples consisted of pH_T and DIC; for the Arctic samples, input consisted of pH_T, TA, and phosphate and silicate concentrations. Sample salinity (S) and pH_T measurement temperature (25 °C) and pressure (1 atm) were provided as input parameters for all calculations.

For the spectrophotometrically based calculations of in situ Ω_{CaCO_3}, shipboard measurements of pH_T (i.e., $-\log[H^+]_T$) were provided to CO2SYS as one input parameter. Ideally, $[CO_3^{2-}]_{Tspec}$ would have served as the other. However, because $[CO_3^{2-}]_T$ is not currently accepted as input for standard CO_2 system calculators,[33,36] it was necessary to first calculate (spectrophotometrically derived) DIC as an alternative input parameter. DIC is defined as:

$$DIC = [CO_2^*] + [HCO_3^-]_T + [CO_3^{2-}]_T \quad (6)$$

where $[CO_2^*]$ is the combined concentration of dissolved CO_2 and carbonic acid ($[CO_2^*] = [CO_2] + [H_2CO_3]$) and $[HCO_3^-]_T$ is the total concentration of bicarbonate ion. Expressing eq 6 in terms of the spectrophotometrically measured quantities $[H^+]_T$ and $[CO_3^{2-}]_T$ yields:

$$DIC = [CO_3^{2-}]_T\left(\frac{[H^+]_T^2 + K_1[H^+]_T + K_1K_2}{K_1K_2}\right) \quad (7)$$

where the equilibrium quotients K_1 and K_2 are defined as:

$$K_1 = [H^+]_T[HCO_3^-]_T/[CO_2^*] \quad (8)$$

$$K_2 = [H^+]_T[CO_3^{2-}]_T/[HCO_3^-]_T \quad (9)$$

The values of K_i (for conditions of sample S, analysis temperature of 25 °C, and analysis pressure of 1 atm) were determined according to the Lueker et al.[37] characterization of the Mehrbach constants on the total pH scale. DIC (eq 7) was then provided as the second input parameter to CO2SYS, which calculated in situ Ω_C and Ω_A. (Supporting Information

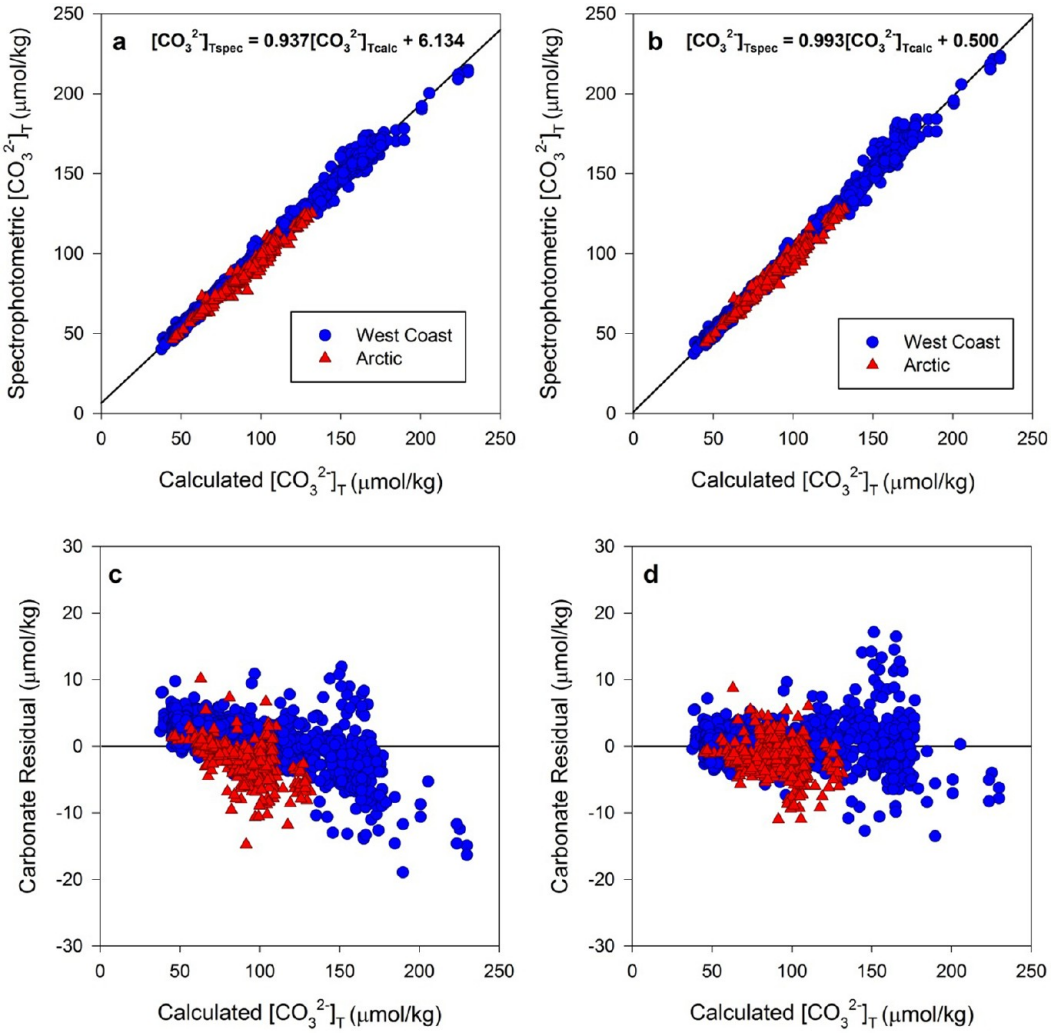

Figure 4. Top panels (a and b): Spectrophotometrically determined carbonate ion concentrations, $[CO_3^{2-}]_{Tspec}$, versus conventionally calculated concentrations, $[CO_3^{2-}]_{Tcalc}$ (at 25 °C). Bottom panels (c and d): Carbonate ion residuals ($[CO_3^{2-}]_{Tspec} - [CO_3^{2-}]_{Tcalc}$) as a function of $[CO_3^{2-}]_{Tcalc}$. The left panels (a and c) use the parametrization of Byrne and Yao[27] (eqs 2−4), whereas the right panels (b and d) use the modeled parameters of this work (eqs 10−12). For (a), the best-fit equation is $[CO_3^{2-}]_{Tspec} = 0.937[CO_3^{2-}]_{Tcalc} + 6.134$, with $r^2 = 0.993$. For (b), the best-fit relationship is $[CO_3^{2-}]_{Tspec} = 0.993[CO_3^{2-}]_{Tcalc} + 0.500$, with $r^2 = 0.994$). The r^2 values are based on a model I linear regression.

for further explanation regarding the selection of thermodynamic equilibrium constants.)

RESULTS AND DISCUSSION

Spectrophotometric Measurement of Total Carbonate Ion Concentrations. Eqs 2−4, which give the parameters required to obtain spectrophotometric $[CO_3^{2-}]_{Tspec}$ from eq 1, were developed from laboratory observations of Pb(II) UV spectra, TA, and potentiometric pH in manipulated natural seawater over a range of laboratory conditions ($[CO_3^{2-}]_T$, S, and pH).[27] Purified pH indicator was not available at the time for the electrode calibrations.[38] Using the 2011 field data (N = 1480, 26.6 ≤ S ≤ 34.9, and 38 ≤ $[CO_3^{2-}]_T$ ≤ 258 μmol kg^{-1} at 25 °C and 1 atm) and purified mCP to extend the laboratory observations and optimize eqs 2−4 yielded these relationships:

$$\log\{({}_{CO_3}\beta_1)/(e_2)\} = 5.513 - 5.358 \times 10^{-2}S + 5.166 \times 10^{-4}S^2 \quad (10)$$

$$e_1 = 0.2293 - 5.554 \times 10^{-4}S + 8.440 \times 10^{-5}S^2 \quad (11)$$

$$(e_3/e_2) = 3.091 - 8.730 \times 10^{-2}S + 9.363 \times 10^{-4}S^2 \quad (12)$$

A comparison of the two sets of parametrizations (eqs 2−4 and eqs 10−12) is shown in Figure 3. The e_3/e_2 parameter required the smallest modification, which is reasonable considering the straightforward manner in which molar absorptivity properties are determined in acidified seawater, with only free Pb(II) and lead chloride species present in solution. The $\log(\beta/e_2)$ and e_1 terms, which describe aspects of lead carbonate formation and absorbance characteristics, require measurements at high pH. The larger differences between the laboratory- and field-modeled $\log(\beta/e_2)$ and e_1 terms illustrate the need for highly accurate potentiometric pH measurements when $[CO_3^{2-}]_T$ parametrizations are developed.[39]

Goodness of model fit is shown in Figure 4. The improved agreement between conventionally calculated $[CO_3^{2-}]_{Tcalc}$ and spectrophotometric $[CO_3^{2-}]_{Tspec}$ obtained with eqs 10−12 is evident in comparisons of the slopes and residuals. The average

dx.doi.org/10.1021/es303631g | Environ. Sci. Technol. 2013, 47, 1468−1477

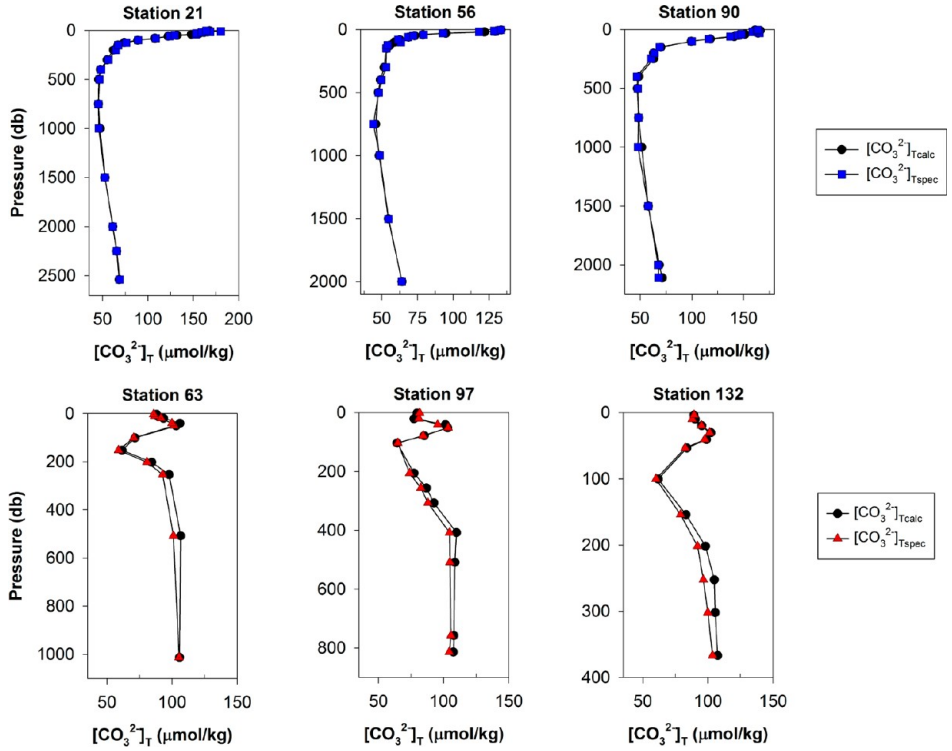

Figure 5. Vertical profiles of $[CO_3^{2-}]_T$ (at 25 °C) from selected stations of the West Coast (upper row) and Arctic Ocean (lower row) cruises. Conventionally calculated $[CO_3^{2-}]_{Tcalc}$ is shown in black, and spectrophotometrically measured $[CO_3^{2-}]_{Tspec}$ is shown in blue (West Coast) or red (Arctic).

absolute residual for samples with $38 \leq [CO_3^{2-}]_T \leq 120$ μmol kg^{-1} decreased from 2.8 to 1.7 μmol kg^{-1}. For samples with $[CO_3^{2-}]_T > 120$ μmol kg^{-1}, the average absolute residual decreased from 4.4 μmol kg^{-1} to 3.5 μmol kg^{-1}. In addition, the generally negative slope defined by the original residuals was eliminated by the optimization, with the new residuals clustering uniformly about $y = 0$. The residual sum of squares was reduced from 22 046 to 12 345. Frequency distributions of the two sets of residuals (Figure S2 of the Supporting Information) show that the negatively skewed distribution obtained with eqs 2−4 approaches a normal distribution with the refined parameter set; the overall improved fit resulted in an r^2 value of 0.995. All subsequent discussion refers to results obtained using the updated spectrochemical model (eqs 1, 10−12).

The overall mean percent difference between the conventionally calculated ($[CO_3^{2-}]_{Tcalc}$) and directly measured ($[CO_3^{2-}]_{Tspec}$) concentrations thus obtained (1480 observations) was 2.30% (SD 1.85%). Approximately 73% of the $[CO_3^{2-}]_{Tspec}$ values fell within 2 μmol kg^{-1} of the $[CO_3^{2-}]_{Tcalc}$ values; 95% fell within 5 μmol kg^{-1}. On the basis of 171 duplicate field samples, the shipboard analytical precision of the $[CO_3^{2-}]_{Tspec}$ method was estimated to be ~1.71 μmol kg^{-1} (2.28%) for the range of carbonate concentrations encountered (~35−220 μmol kg^{-1}).

Carbonate Concentration Profiles. Vertical profiles of directly measured $[CO_3^{2-}]_{Tspec}$ are shown in Figure 5, along with profiles of conventionally calculated $[CO_3^{2-}]_{Tcalc}$. In the North Pacific (top panels), $[CO_3^{2-}]_T$ gradually decreased with depth from the surface through the euphotic zone. At depths >500 m, $[CO_3^{2-}]_T$ increased, consistent with in situ dissolution of solid $CaCO_3$.[11] In the Arctic basin (bottom panels), the upper ocean $[CO_3^{2-}]_T$ profiles reflect the region's complex physical and biological processes.[40,41] The offsets between Arctic $[CO_3^{2-}]_{Tspec}$ and $[CO_3^{2-}]_{Tcalc}$ at depth are consistent with the typical magnitudes of the residuals shown in part d of Figure 4. In addition to contributions from imprecision in the spectrophotometric measurements, some portion of the offsets could be due to small errors associated with the use of TA rather than DIC for the calculations of $[CO_3^{2-}]_{Tcalc}$. The pH_T−DIC combination is a more direct approach for calculating $[CO_3^{2-}]_T$. Calculations via the pH_T−TA pair could, for

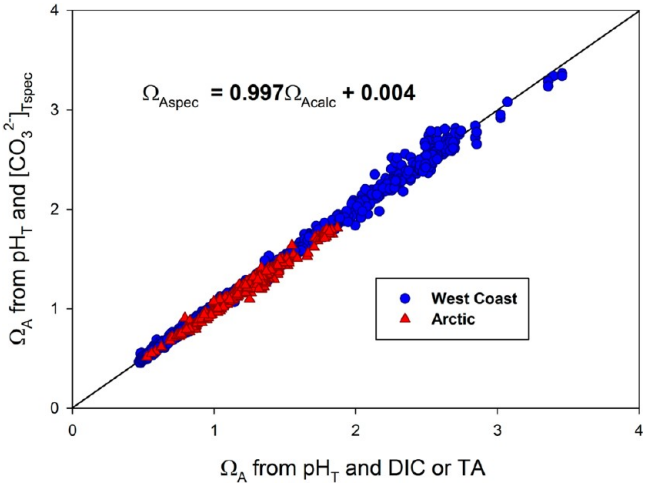

Figure 6. Aragonite saturation states (Ω_A) at in situ temperature and pressure, obtained spectrophotometrically (from pH_T−$[CO_3^{2-}]_{Tspec}$) and conventionally (from pH_T−DIC or pH_T−TA). The best-fit relationship (black line) between Ω_{Aspec} and Ω_{Acalc} is given as $\Omega_{Aspec} = 0.997\Omega_{Acalc} + 0.004$ ($r^2 = 0.996$).

dx.doi.org/10.1021/es303631g | Environ. Sci. Technol. 2013, 47, 1468−1477

Table 1. Comparison of Conventionally Calculated (Ω_{Acalc}) and Spectrophotometrically Based (Ω_{Aspec}) in Situ Aragonite Saturation States; for Each Increment of Ω_{Acalc}, the Number of Samples (N) Is Given, along with the Average Difference between Ω_{Aspec} and Ω_{Acalc} in Each Confidence Interval (CI)

percentage of samples (CI)	Ω_A = 0.5−1.0 (N = 699)	Ω_A = 1.0−1.5 (N = 404)	Ω_A = 1.5−2.0 (N = 167)	Ω_A = 2.0−2.5 (N = 130)	Ω_A = 2.5−3.0 (N = 72)	Ω_A = 3.0−3.5 (N = 8)
67%	±0.02	±0.04	±0.04	±0.06	±0.07	±0.13
95%	±0.05	±0.07	±0.09	±0.18	±0.19	±0.13
99%	±0.06	±0.12	±0.11	±0.21	±0.22	±0.13
100%	±0.12	±0.15	±0.13	±0.25	±0.24	±0.13

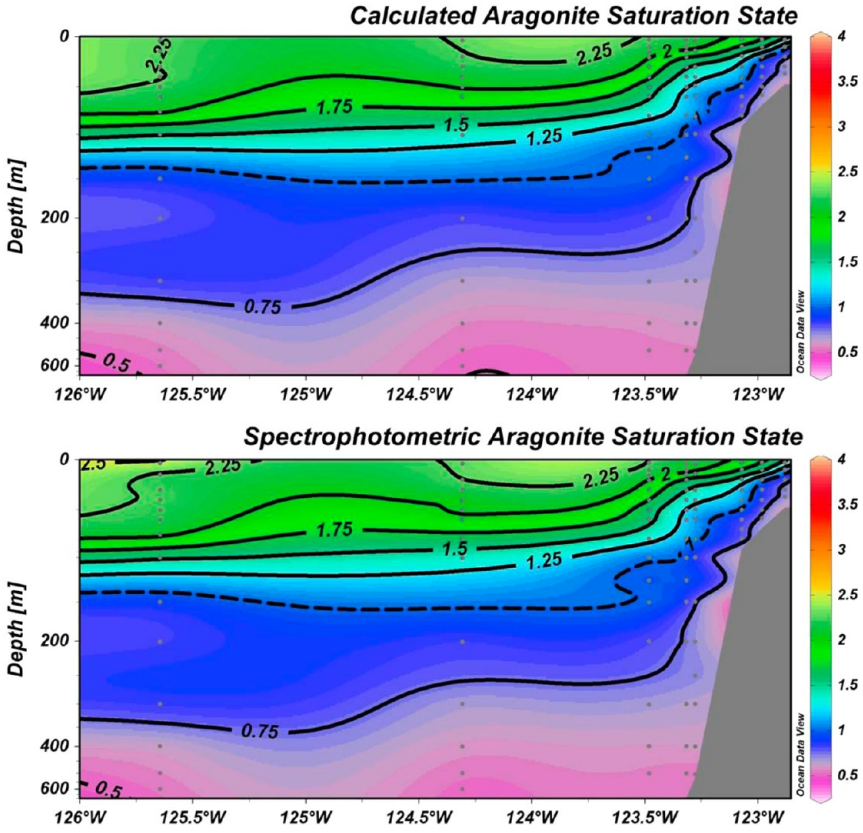

Figure 7. Cross sections of in situ aragonite saturation state off the coast of San Francisco, California (West Coast line 10, Figure 2). The top panel shows Ω_{Acalc}, obtained from conventional shipboard measurements of pH_T and DIC. The lower panel shows Ω_{Aspec}, obtained from spectrophotometric measurements of pH_T and $[CO_3^{2-}]_{Tspec}$. The dashed line indicates saturation state equal to 1. An expanded view of surface waters near the shelf break can be found in Figure S4 of the Supporting Information.

example, be influenced by the presence of protolytes associated with dissolved organic carbon and particulate organic carbon, both of which can be elevated in coastal Arctic waters due to riverine influences.[20,42−44]

Calcium Carbonate Saturation States. Aragonite saturation states (Ω_A) obtained from the spectrophotometric measurements of pH_T and $[CO_3^{2-}]_T$ are shown in Figure 6 as Ω_{Aspec}, along with conventionally calculated Ω_{Acalc}. Results of the two approaches demonstrate a high level of agreement. The larger deviations between $[CO_3^{2-}]_{Tspec}$ and $[CO_3^{2-}]_{Tcalc}$ for $[CO_3^{2-}]_T > 150$ μmol kg^{-1} (part d of Figure 4) are evident in the comparison of aragonite saturation states: for samples with a lower saturation state, $0.5 \leq \Omega_{Acalc} \leq 2.0$, the 95% confidence interval (CI) for in situ saturation state is 0.06; for samples with $\Omega_{Acalc} > 2.0$, the 95% CI is 0.18 (Table 1). Representative cross sections of Ω_A (Figure 7 and Figure S4 of the Supporting Information) reveal areas of undersaturated waters ($\Omega_A < 1$) on the continental shelf[45,46] (below ∼10 m, ∼17 m, and ∼40 m, for the three stations nearest the coast). The condition of undersaturation has been shown to adversely affect the larval stages of oysters,[47] clams,[48] and pteropods.[49,50] Figures S4 and S5 of the Supporting Information show similar assessments of calcite saturation state, Ω_C.

Implications. This work presents the first shipboard investigations of the use of Pb(II) UV spectroscopy to directly measure carbonate ion concentrations at sea. Field data from two cruises, one along the U.S. West Coast and one in Arctic waters, provided a range of oceanographic conditions (S, temperature, and $[CO_3^{2-}]_T$) to test the method in the field. As first presented by Byrne and Yao,[27] the Pb(II) approach demonstrated good laboratory agreement with standard methods for calculating $[CO_3^{2-}]_T$, but the authors noted several limitations in their characterization of the fitting parameters (eqs 2−4). Their electrode calibrations, for example, were performed using unpurified thymol blue indicator.[51] Our measurements confirm their suspicions that the parameters would perhaps require refinement. Small revisions (eqs 10−12), particularly of the log (β/e_2) and e_1

dx.doi.org/10.1021/es303631g | Environ. Sci. Technol. 2013, 47, 1468−1477

terms, substantially improved agreement between spectrophotometrically measured and conventionally calculated $[CO_3^{2-}]_T$, especially at higher concentrations. With the refined model, nearly three-fourths of the $[CO_3^{2-}]_{Tspec}$ samples were within 2 μmol kg^{-1} of $[CO_3^{2-}]_{Tcalc}$.

Our findings indicate that the straightforward and relatively inexpensive Pb(II) method can be conveniently and reliably used at sea and in other challenging settings. This capability may be of particular value to facilities without the specialized coulometric and titrimetric instrumentation needed to measure DIC and TA. The spectrophotometric approach can be used for routine seawater monitoring, for example, on research ships or at onshore shellfish hatcheries.[48,49] For spectrophotometric pH_T and $[CO_3^{2-}]_T$ measurements, the only instrumentation required is a thermostatted spectrophotometer. Discrete seawater samples are collected directly into 10 cm optical cells for analysis. The primary reagents are indicator dye (purified mCP) and $PbCl_2$ titrant. Simple models relating pH_T and $[CO_3^{2-}]_T$ to the absorbance and thermodynamic properties of mCP and Pb(II) enable calibration-free determinations of carbonate saturation states in seawater.

Carbonate ion concentration, $[CO_3^{2-}]_T$, is now well positioned to serve as a fifth independently measured parameter to complement the established quartet of pH, DIC, TA, and fCO_2. Laboratory and shipboard development of the Pb(II) spectrochemical model is ongoing, and improvements in precision can be expected as the method matures. The characterizations expressed in eqs 1 and 10−12 are based on the most extensive (laboratory plus field) data currently available. In the future, as additional multiparameter data sets are acquired and as carbonate concentration standards are developed (none exist at present), it will be possible to assess the accuracy of the $[CO_3^{2-}]_{Tspec}$ method as well as its utility for calculating other carbon-system parameters. Model refinements may be warranted. Researchers utilizing spectrophotometric methods to characterize seawater chemistry should routinely archive absorbance ratios (R) so that $[CO_3^{2-}]_T$ values can be refined via subsequent improvements in the modeled absorbance behavior of Pb(II).

Automated spectrophotometric techniques offer fast, high-precision capabilities for long-term monitoring in situ. Autonomous spectrophotometric pH sensors are currently being used on moorings and are being considered for use on profiling floats and gliders.[52] When additional carbon-system sensors are eventually added, use of spectrophotometric sensor(s) for the complementary measurements (e.g., DIC,[53,54] $[CO_3^{2-}]_T$) will simplify instrumental integration. The direct $[CO_3^{2-}]_T$ measurement model embodied in eqs 1 and 10−12 is currently being extended to enable observations over a range of temperatures and pressures. Our measurements at low to moderate carbonate ion concentrations in the Pacific and Arctic Oceans constitute an important first step in the development and validation of procedures for direct in situ measurements of carbonate ion concentrations.

■ ASSOCIATED CONTENT

Supporting Information

Details regarding the selection of thermodynamic equilibrium constants. Additional figures are also included to show carbonate ion perturbation trends, frequency distributions of model residuals, and calcium carbonate saturation state comparisons. This material is available free of charge via the Internet at http://pubs.acs.org.

■ AUTHOR INFORMATION

Corresponding Author

*Phone: +1-727-553-1508, fax: +1-727-553-1189, e-mail: rhbyrne@usf.edu.

Notes

The authors declare no competing financial interest.

■ ACKNOWLEDGMENTS

This work was supported by NSF Awards OCE-0927108 (RHB), OCE-0727082 (RHB), and ARC1041102 (JTM), as well as NOAA Awards NA110AR4320199 (USM-GR04148-003), and NA080AR432075 (UAF 11-0027). We would like to thank Bo Yang, Jian Ma, Xioling Ding, and Matthew Elliot of the University of South Florida College of Marine Science for their assistance in collecting and analyzing the field samples. We would like to thank the Associate Editor and three anonymous reviewers for their helpful suggestions. The insightful editorial guidance provided by Dr. Tonya Clayton is greatly appreciated.

■ REFERENCES

(1) Caldeira, K.; Wickett, M. E. Ocean model predictions of chemistry changes from carbon dioxide emissions to the atmosphere and ocean. *J. Geophys. Res.* **2005**, *110* (C9), C09S04.

(2) Caldeira, K.; Wickett, M. E. Oceanography: Anthropogenic carbon and ocean pH. *Nature* **2003**, *425* (6956), 365−365.

(3) Feely, R. A.; Doney, S. C.; Cooley, S. R. Ocean acidification: Present conditions and future changes in a high-CO_2 world. *Oceanography* **2009**, *22* (4), 36−47.

(4) Fabry, V. J.; Seibel, B. A.; Feely, R. A.; Orr, J. C. Impacts of ocean acidification on marine fauna and ecosystem processes. *ICES J. Mar. Sci.* **2008**, *65* (3), 414−432.

(5) Doney, S. C.; Ruckelshaus, M.; Emmett Duffy, J.; Barry, J. P.; Chan, F.; English, C. A.; Galindo, H. M.; Grebmeier, J. M.; Hollowed, A. B.; Knowlton, N.; Polovina, J.; Rabalais, N. N.; Sydeman, W. J.; Talley, L. D. Climate change impacts on marine ecosystems. *Annu. Rev. Mar. Sci.* **2012**, *4* (1), 11−37.

(6) Ferrari, M. C. O.; Manassa, R. P.; Dixson, D. L.; Munday, P. L.; McCormick, M. I.; Meekan, M. G.; Sih, A.; Chivers, D. P. Effects of ocean acidification on learning in coral reef fishes. *PLoS ONE* **2012**, *7* (2), e31478.

(7) Abbasi, T.; Abbasi, S. A. Ocean acidification: The newest threat to the global environment. *Crit. Rev. Environ. Sci. Technol.* **2011**, *41* (18), 1601−1663.

(8) Newbold, L. K.; Oliver, A. E.; Booth, T.; Tiwari, B.; DeSantis, T.; Maguire, M.; Andersen, G.; van der Gast, C. J.; Whiteley, A. S. The response of marine picoplankton to ocean acidification. *Environ. Microbiol.* **2012**, *14* (9), 2293−2307.

(9) Hofmann, G. E.; Smith, J. E.; Johnson, K. S.; Send, U.; Levin, L. A.; Micheli, F.; Paytan, A.; Price, N. N.; Peterson, B.; Takeshita, Y.; Matson, P. G.; Crook, E. D.; Kroeker, K. J.; Gambi, M. C.; Rivest, E. B.; Frieder, C. A.; Yu, P. C.; Martz, T. R. High-frequency dynamics of ocean pH: A multi-ecosystem comparison. *PLoS ONE* **2011**, *6* (12), e28983.

(10) Feely, R. A.; Sabine, C. L.; Byrne, R. H.; Millero, F. J.; Dickson, A. G.; Wanninkhof, R.; Murata, A.; Miller, L. A.; Greeley, D. Decadal changes in the aragonite and calcite saturation state of the Pacific Ocean. *Global Biogeochem. Cycles* **2012**, *26* (3), GB3001.

(11) Feely, R. A.; Sabine, C. L.; Lee, K.; Berelson, W.; Kleypas, J.; Fabry, V. J.; Millero, F. J. Impact of anthropogenic CO_2 on the $CaCO_3$ system in the oceans. *Science* **2004**, *305* (5682), 362−366.

(12) Orr, J. C.; Fabry, V. J.; Aumont, O.; Bopp, L.; Doney, S. C.; Feely, R. A.; Gnanadesikan, A.; Gruber, N.; Ishida, A.; Joos, F.; Key, R. M.; Lindsay, K.; Maier-Reimer, E.; Matear, R.; Monfray, P.; Mouchet, A.; Najjar, R. G.; Plattner, G.-K.; Rodgers, K. B.; Sabine, C. L.; Sarmiento, J. L.; Schlitzer, R.; Slater, R. D.; Totterdell, I. J.; Weirig, M.-

F.; Yamanaka, Y.; Yool, A. Anthropogenic ocean acidification over the twenty-first century and its impact on calcifying organisms. *Nature* **2005**, *437* (7059), 681−686.
(13) Iglesias-Rodriguez, M. D.; Halloran, P. R.; Rickaby, R. E. M.; Hall, I. R.; Colmenero-Hidalgo, E.; Gittins, J. R.; Green, D. R. H.; Tyrrell, T.; Gibbs, S. J.; von Dassow, P.; Rehm, E.; Armbrust, E. V.; Boessenkool, K. P. Phytoplankton calcification in a high-CO_2 world. *Science* **2008**, *320* (5874), 336−340.
(14) Moy, A. D.; Howard, W. R.; Bray, S. G.; Trull, T. W. Reduced calcification in modern Southern Ocean planktonic foraminifera. *Nature Geosci.* **2009**, *2* (4), 276−280.
(15) Cooley, S. R.; Doney, S. C. Anticipating ocean acidification's economic consequences for commercial fisheries. *Environ. Res. Lett.* **2009**, *4* (2), 024007.
(16) Cheung, W. W. L.; Dunne, J.; Sarmiento, J. L.; Pauly, D. Integrating ecophysiology and plankton dynamics into projected maximum fisheries catch potential under climate change in the Northeast Atlantic. *ICES J. Mar. Sci.* **2011**, *68* (6), 1008−1018.
(17) Mathis, J. T.; Cross, J. N.; Bates, N. R. Coupling primary production and terrestrial runoff to ocean acidification and carbonate mineral suppression in the eastern Bering Sea. *J. Geophys. Res.* **2011**, *116* (C2), C02030.
(18) Yamamoto-Kawai, M.; McLaughlin, F. A.; Carmack, E. C.; Nishino, S.; Shimada, K. Aragonite undersaturation in the Arctic Ocean: Effects of ocean acidification and sea ice melt. *Science* **2009**, *326* (5956), 1098−1100.
(19) Hansell, D. A.; Kadko, D.; Bates, N. R. Degradation of terrigenous dissolved organic carbon in the western Arctic Ocean. *Science* **2004**, *304* (5672), 858−861.
(20) Letscher, R. T.; Hansell, D. A.; Kadko, D. Rapid removal of terrigenous dissolved organic carbon over the Eurasian shelves of the Arctic Ocean. *Mar. Chem* **2011**, *123* (1−4), 78−87.
(21) Mathis, J. T.; Cross, J. N.; Bates, N. R. The role of ocean acidification in systemic carbonate mineral suppression in the Bering Sea. *Geophys. Res. Lett.* **2011**, *38* (19), L19602.
(22) Dickson, A. G.; Sabine, C. L.; Christian, J. R. *Guide to Best Practices for Ocean CO_2 Measurements*; PICES Special Publication 3, 2007.
(23) Riebesell, U.; Fabry, V. J.; Hansson, L.; Gattuso, J.-P. *Guide to Best Practices for Ocean Acidification Research and Data Reporting*; Publications Office of the European Union: Luxembourg, 2010.
(24) Choi, Y. S.; Lvova, L.; Shin, J. H.; Oh, S. H.; Lee, C. S.; Kim, B. H.; Cha, G. S.; Nam, H. Determination of oceanic carbon dioxide using a carbonate-selective electrode. *Anal. Chem.* **2002**, *74* (10), 2435−2440.
(25) Makarychev-Mikhailov, S.; Legin, A.; Mortensen, J.; Levitchev, S.; Vlasov, Y. Potentiometric and theoretical studies of the carbonate sensors based on 3-bromo-4-hexyl-5-nitrotrifluoroacetophenone. *Analyst* **2004**, *129* (3), 213−218.
(26) Martz, T. R.; Jannasch, H. W.; Johnson, K. S. Determination of carbonate ion concentration and inner sphere carbonate ion pairs in seawater by ultraviolet spectrophotometric titration. *Mar. Chem.* **2009**, *115* (3−4), 145−154.
(27) Byrne, R. H.; Yao, W. Procedures for measurement of carbonate ion concentrations in seawater by direct spectrophotometric observations of Pb(II) complexation. *Mar. Chem.* **2008**, *112* (1−2), 128−135.
(28) Liu, X.; Patsavas, M. C.; Byrne, R. H. Purification and characterization of meta-cresol purple for spectrophotometric seawater pH measurements. *Environ. Sci. Technol.* **2011**, *45* (11), 4862−4868.
(29) Yao, W.; Byrne, R. H. Simplified seawater alkalinity analysis: Use of linear array spectrometers. *Deep Sea Res. Part I Oceanogr. Res. Pap.* **1998**, *45* (8), 1383−1392.
(30) Dickson, A. G. Standards for ocean measurements. *Oceanography* **2010**, *23* (3), 34−47.
(31) Dore, J. E.; Houlihan, T.; Hebel, D. V.; Tien, G.; Tupas, L.; Karl, D. M. Freezing as a method of sample preservation for the analysis of dissolved inorganic nutrients in seawater. *Mar. Chem.* **1996**, *53* (3−4), 173−185.
(32) Clayton, T. D.; Byrne, R. H. Spectrophotometric seawater pH measurements: total hydrogen ion concentration scale calibration of m-cresol purple and at-sea results. *Deep Sea Res. Part I Oceanogr. Res. Pap.* **1993**, *40* (10), 2115−2129.
(33) Pierrot, D. E.; Lewis, E.; Wallace, D. W. R. "*MS Excel Program Developed for CO_2 System Calculations*," Carbon Dioxide Information Analysis Center, Oak Ridge National Laboratory, U.S. Department of Energy, 2006.
(34) Mehrbach, C.; Culberson, C. H.; Hawley, J. E.; Pytkowicz, R. M. Measurement of the apparent dissociation constants of carbonic acid in seawater at atmospheric pressure. *Limnol. Oceanogr.* **1973**, *18* (6), 897−907.
(35) Dickson, A. G.; Millero, F. J. A comparison of the equilibrium constants for the dissociation of carbonic acid in seawater media. *Deep Sea Res. Part A Oceanogr. Res. Pap.* **1987**, *34* (10), 1733−1743.
(36) Robbins, L. L.; Hansen, M. E.; Kleypas, J. A.; Meylan, S. C. "CO2calc—A user-friendly seawater carbon calculator for Windows, Max OS X, and iOS (iPhone)," USGS Open-File Report 2010−1280 17 p., 2010.
(37) Lueker, T. J.; Dickson, A. G.; Keeling, C. D. Ocean pCO_2 calculated from dissolved inorganic carbon, alkalinity, and equations for K_1 and K_2: Validation based on laboratory measurements of CO_2 in gas and seawater at equilibrium. *Mar. Chem* **2000**, *70* (1−3), 105−119.
(38) Yao, W.; Liu, X.; Byrne, R. H. Impurities in indicators used for spectrophotometric seawater pH measurements: Assessment and remedies. *Mar. Chem.* **2007**, *107* (2), 167−172.
(39) Easley, R. A.; Byrne, R. H. Spectrophotometric calibration of pH electrodes in seawater using purified m-cresol purple. *Environ. Sci. Technol.* **2012**, *46* (9), 5018−5024.
(40) Mathis, J. T.; Pickart, R. S.; Byrne, R. H.; McNeil, C. L.; Moore, G. W. K.; Juranek, L. W.; Liu, X.; Ma, J.; Easley, R. A.; Elliot, M. M.; Cross, J. N.; Reisdorph, S. C.; Bahr, F.; Morison, J.; Lichendorf, T.; Feely, R. A. Storm-induced upwelling of high pCO_2 waters onto the continental shelf of the western Arctic Ocean and implications for carbonate mineral saturation states. *Geophys. Res. Lett.* **2012**, *39* (7), L07606.
(41) Schulze, L. M.; Pickart, R. S. Seasonal variation of upwelling in the Alaskan Beaufort Sea: Impact of sea ice cover. *J. Geophys. Res.* **2012**, *117* (C6), C06022.
(42) Millero, F.; Huang, F.; Woosley, R.; Letscher, R.; Hansell, D. Effect of dissolved organic carbon and alkalinity on the density of arctic ocean waters. *Aquat. Geochem.* **2011**, *17* (4), 311−326.
(43) Anderson, L. G.; Jutterström, S.; Kaltin, S.; Jones, E. P.; Björk, G. Variability in river runoff distribution in the Eurasian Basin of the Arctic Ocean. *J. Geophys. Res.* **2004**, *109* (C1), C01016.
(44) Mathis, J. T.; Pickart, R. S.; Hansell, D. A.; Kadko, D.; Bates, N. R. Eddy transport of organic carbon and nutrients from the Chukchi Shelf: Impact on the upper halocline of the western Arctic Ocean. *J. Geophys. Res.* **2007**, *112* (C5), C05011.
(45) Feely, R. A.; Sabine, C. L.; Hernandez-Ayon, J. M.; Ianson, D.; Hales, B. Evidence for upwelling of corrosive "acidified" water onto the continental shelf. *Science* **2008**, *320* (5882), 1490−1492.
(46) Gruber, N.; Hauri, C.; Lachkar, Z.; Loher, D.; Frölicher, T. L.; Plattner, G.-K. Rapid progression of ocean acidification in the California Current System. *Science* **2012**, *337* (6091), 220−223.
(47) Barton, A.; Hales, B.; Waldbusser, G. G.; Langdon, C.; Feely, R. A. The Pacific oyster, Crassostrea gigas, shows negative correlation to naturally elevated carbon dioxide levels: Implications for near-term ocean acidification effects. *Limnol. Oceanogr.* **2012**, *57* (3), 698−710.
(48) Range, P.; Chícharo, M. A.; Ben-Hamadou, R.; Piló, D.; Matias, D.; Joaquim, S.; Oliveira, A. P.; Chícharo, L. Calcification, growth and mortality of juvenile clams Ruditapes decussatus under increased pCO_2 and reduced pH: Variable responses to ocean acidification at local scales? *J. Exper. Marine Biology and Ecology* **2011**, *396* (2), 177−184.
(49) Comeau, S.; Gattuso, J.-P.; Nisumaa, A.-M.; Orr, J. Impact of aragonite saturation state changes on migratory pteropods. *Proc. Royal Soc. B: Biol. Sci.* **2012**, *279* (1729), 732−738.

(50) Comeau, S.; Gorsky, G.; Alliouane, S.; Gattuso, J. P. Larvae of the pteropod Cavolinia inflexa exposed to aragonite undersaturation are viable but shell-less. *Mar. Biol.* **2010**, *157* (10), 2341−2345.
(51) Zhang, H.; Byrne, R. H. Spectrophotometric pH measurements of surface seawater at in-situ conditions: absorbance and protonation behavior of thymol blue. *Mar. Chem.* **1996**, *52* (1), 17−25.
(52) Johnson, K. S.; Berelson, W. M.; Boss, E. S.; Chase, Z.; Claustre, H.; Emerson, S. R.; Gruber, N.; Kortzinger, A.; Perry, M. J.; Riser, S. C. Observing biogeochemical cycles at global scales with profiling floats and gliders: Prospects for a global array. *Oceanography* **2009**, *22* (3), 216−225.
(53) Byrne, R. H.; Liu, X.; Kaltenbacher, E. A.; Sell, K. Spectrophotometric measurement of total inorganic carbon in aqueous solutions using a liquid core waveguide. *Anal. Chim. Acta* **2002**, *451* (2), 221−229.
(54) Wang, Z. A.; Liu, X.; Byrne, R. H.; Wanninkhof, R.; Bernstein, R. E.; Kaltenbacher, E. A.; Patten, J. Simultaneous spectrophotometric flow-through measurements of pH, carbon dioxide fugacity, and total inorganic carbon in seawater. *Anal. Chim. Acta* **2007**, *596* (1), 23−36.